



OPEN

# Inhibitory effects of high extracellular L-glutamate concentrations on skeletal myogenesis

Himiko Ban<sup>1,2</sup>, Koji Nobe<sup>1,2</sup> & Soushi Kobayashi<sup>1,2</sup>✉

L-glutamate (Glu) is accumulated abundantly in skeletal muscle cells and plays a central role in energy production, amino acid metabolism, and protein synthesis. If intracellular Glu leaks due to plasma membrane fragility or injury, it may adversely affect the surrounding myocytes. In the present study, we examined the effects of high extracellular Glu concentration on skeletal myogenesis. Five mM Glu stimulation decreased the expression of fast-twitch myosin heavy chain isoforms and myogenin, an indicator of C2C12 cell differentiation into myocytes, and inhibited the cell fusion. This stimulation reduced the expression of metabotropic glutamate receptor 5 (mGluR5) and *N*-methyl-D-aspartate receptor 1 (NMDAR), which are glutamate receptors on the C2C12 plasma membrane. Furthermore, phosphorylation of p38 mitogen-activated protein kinase, myocyte enhancer factor 2A, and cAMP response element binding protein, which are downstream of these Glu receptors, was reduced, and the expression of peroxisome proliferator-activated receptor gamma coactivator 1-alpha (PGC-1α) decreased. Moreover, reduced mGluR5 and NMDAR expression and muscle weight were observed in the tibialis anterior muscle of mice with increased aging markers. These findings provide insights into the molecular mechanisms contributing to age-related muscle fragility and highlight the potential detrimental effects of elevated Glu on muscle health.

**Keywords** C2C12, Glutamate receptor, L-glutamate, Myogenesis, Skeletal muscle

Muscle tissue is classified into three different types—cardiac, skeletal, and smooth—and accounts for approximately half of the body weight. Skeletal muscle, which comprises most of the muscle tissue, plays a crucial role in energy metabolism, blood glucose uptake, and physical activity. Skeletal muscle consists of bundles of muscle fibers formed by the fusion of mononuclear myocytes differentiated from myoblasts. Following an injury to the skeletal muscle, satellite cells are activated, giving rise to proliferating myoblasts that promote skeletal muscle regeneration<sup>1,2</sup>.

L-glutamate (Glu) is an acidic amino acid synthesized from glutamine in most cells<sup>3</sup>. It is essential not only for protein synthesis but also for energy production and amino acid metabolism<sup>4</sup>. The role of Glu in the central nervous system has been studied in detail, where it is released from the axon terminus and the extracellular Glu modulates brain excitability, learning, memory and psychomotor behavior via Glu receptors<sup>5</sup>. However, excess extracellular Glu causes excitotoxicity, leading to ischemia, traumatic brain injury, and chronic neurodegenerative diseases<sup>6</sup>. Glu is highly abundant in skeletal muscle cells and plays a central role in the energy supply during exercise by facilitating tricarboxylic acid (TCA) cycle and nucleotide metabolism<sup>7,8</sup>. Skeletal muscle cells do not secrete Glu in a manner similar to neurons but are exposed to Glu from the blood supply. The effects of both physiological and excess extracellular Glu on these cells remain poorly understood.

Glu receptors are expressed on the plasma membrane and are classified as metabolic Glu receptors, which are G protein-coupled and cation channel-coupled receptors<sup>9</sup>. The former are classified into three groups based on sequence homology, G protein binding, and ligand selectivity. Group I (mGluR1 and mGluR5) stimulate phospholipase C and adenylyl cyclase activity, as well as MAP kinase phosphorylation. Group II (mGluR2 and mGluR3) reduces the activity of adenylyl cyclase and Ca<sup>2+</sup> channels while promoting the activity of K<sup>+</sup> channels. Group III (mGluR4, mGluR6, mGluR7, and mGluR8) functions similarly to group II and has a high affinity for the orthosteric agonist L-AP4. Cation channel-coupled receptors are classified as *N*-methyl-D-aspartate

<sup>1</sup>Department of Pharmacology, Showa Medical University, 1-5-8 Hatanodai, Shinagawa-ku, Tokyo 142-8555, Japan. <sup>2</sup>Pharmacological Research Center, Showa Medical University, 1-5-8 Hatanodai, Shinagawa-ku, Tokyo 142-8555, Japan. ✉email: soushik@pharm.showa-u.ac.jp

receptors (NMDAR), alpha-amino-3-hydroxyl-5-methyl-4-isoxazole-propionate receptors (AMPA), and kainic acid receptors. mGluR5 and NMDAR are primarily expressed in skeletal muscles, and are associated with its growth<sup>9–11</sup>; however, their detailed functions in skeletal myogenesis remain poorly understood. In contrast, AMPAR and kainic acid receptors are rarely expressed in skeletal muscles<sup>11</sup>. In skeletal muscle, extracellular Glu not only binds to Glu receptors but also regulates both intracellular and extracellular Glu levels via the excitatory amino acid transporter (EAAT) 3, a member of the five EAAT families<sup>12–14</sup>.

When myocytes are injured by stimuli, such as eccentric exercise<sup>15</sup>, intracellular Glu can leak, exposing the surrounding myocytes to high concentrations of Glu. In the present study, we found that a high concentration of Glu inhibited differentiation and fusion of mouse skeletal myoblasts C2C12, which are key processes in myogenesis. Decreased expression of mGluR5 and NMDAR was accompanied by inhibition of their downstream signaling. Furthermore, the expression of these Glu receptors and muscle weight were decreased in the tibialis anterior (TA) muscles of mice with elevated levels of aging marker proteins. Impaired myogenesis may lead to the loss of skeletal muscle mass with aging<sup>16</sup>, suggesting that high levels of Glu may contribute to age-related muscle weakness.

## Results

### Myocyte injury increases extracellular Glu

Most amino acids are present at much higher concentrations in the cytoplasm than in plasma<sup>17</sup>. The cytoplasmic concentration of Glu in human primary myotubes has been reported to be around 16 mM<sup>7</sup>. To determine the intracellular Glu concentration in C2C12 cells, cell lysates were prepared in individual wells of a 96-well plate. When cells per well were lysed with 200  $\mu$ L of lysis buffer, the Glu concentration in the lysate was  $20.5 \pm 0.87 \mu$ M (Fig. 1A). The number of the cells per well was  $60,125 \pm 4279$ . The volume per cell was  $3.3 \times 10^{-9} \pm 5.4 \times 10^{-11}$  mL, and the concentration of Glu per cell was calculated to be  $20.7 \pm 0.87$  mM (Fig. S1). To examine whether the intracellular Glu concentration changed during the early stages of differentiation into myocytes, C2C12 cells were cultured in differentiation medium, and the Glu levels in the cell lysate were measured on days 1–3. Glu concentration in C2C12 cells during differentiation into myocytes decreased on day 1 of differentiation induction and remained unchanged until day 3. However, this concentration was maintained at a high level of 15–26 mM per cell (Fig. S1). In contrast, Glu levels in the differentiation medium increased over the course of C2C12 culture, reaching  $28.9 \pm 1.57 \mu$ M by day 3 of differentiation (Fig. 1B). During myocyte differentiation, some C2C12 cells fail to differentiate undergo apoptosis<sup>18</sup>. In the present study, the percentage of apoptotic cells increased as differentiation progressed (Fig. 1C,D). To determine whether plasma membrane damage occurred during C2C12 differentiation, we examined the percentage of cells with damaged plasma membrane using propidium iodide (PI), a marker for cells with membrane damage. We found that this percentage increased (Fig. 1C,E). To determine whether damage to the plasma membrane causes the abundant intracellular Glu to leak out of the cell, myocytes during differentiation were physically injured using the point of a pipette tip. In this process, a 12-channel pipette was used to equally stimulate the cells in all wells. The cells were cultured in a single row of a 96 well plate, and using a 12-channel pipette, uniform stimulation was applied to all the wells. Glu concentration in the medium after cell injury was found to be higher than that in the control medium containing intact cells (Fig. 1F).

### High Glu concentrations suppresses the expression of fast-twitch myosin heavy chain (MHC) isoforms during the early stages of C2C12 differentiation

When myocytes are injured, intracellular Glu would leak out and diffuse into the original cell space and intercellular spaces. Intracellular fluid constitutes approximately 67% of total body water, while interstitial fluid accounts for approximately 23%<sup>19</sup>. Thus, based on these proportions, cells surrounding the injured myocytes could be exposed to approximately 0.74 times the intracellular concentration of Glu. As noted above, myocytes were calculated to accumulate 15–26 mM Glu per cell during the early stages of differentiation (days 1–3) (Fig. S1), suggesting that the surrounding cells are exposed to 11.1–19.2 mM Glu when a single myocyte is injured. To elucidate the effect of high Glu concentrations during the early stages of differentiation, C2C12 cells were stimulated with 0–30 mM Glu at the start of differentiation and cultured for 3 days. Cytotoxicity was observed at 10–30 mM Glu (Fig. S2). As a result, the maximum concentration of Glu was set at 5 mM. After stimulation with Glu, myosin heavy chain (MHC) and myogenin expression, an indicator of myoblast to myocyte differentiation, was analyzed<sup>20,21</sup>. Based on differences in the MHC subtypes expressed, skeletal muscle fibers are broadly classified into two types: slow-twitch (type I) fibers, which sustain prolonged activity, and fast-twitch (type II) fibers, which contract rapidly and generate large forces<sup>22</sup>. The expression levels of several fast-twitch MHC isoforms (MHCIx, MHCIa, and MHCIb) in C2C12 cells were examined using an anti-Skeletal Muscle Myosin (F59) [we refer to these MHC isoforms as MHC (F59)]. Myogenin is a transcription factor that plays a crucial role from the early stages of myocytes differentiation through the fusion process<sup>21</sup>. On day 2 of differentiation, the expression of these MHC isoforms was increased by 0.3 mM Glu stimulation, a concentration close to physiological blood levels, and significantly decreased by 5 mM Glu, a concentration assuming Glu leakage from neighboring myocytes (Figs. 2A,B and S3). The expression level of MHCIx alone was also reduced by 5 mM Glu (Figs. 2A,C and S3). In contrast, the expression level of slow-twitch MHCI was unchanged by both 0.3 and 5 mM Glu (Figs. 2A,D and S3). The expression of myogenin was decreased in a Glu concentration-dependent manner (Figs. 2E,F and S4). The ratio of MHC (F59)-positive cells (MHC<sup>+</sup>) to MHC (F59)-negative cells (MHC<sup>−</sup>) was also analyzed by immunofluorescence, and 5 mM Glu decreased the percentage of MHC<sup>+</sup> cells (Fig. 2G,H).

### High Glu concentration inhibits C2C12 cell fusion

Myoblasts expressing MHC mature into myotubes through cell fusion<sup>1</sup>. To clarify the effect of high concentrations Glu on the fusion process of C2C12 cells, cells differentiated for 3 days in the presence of 0–5 mM Glu were

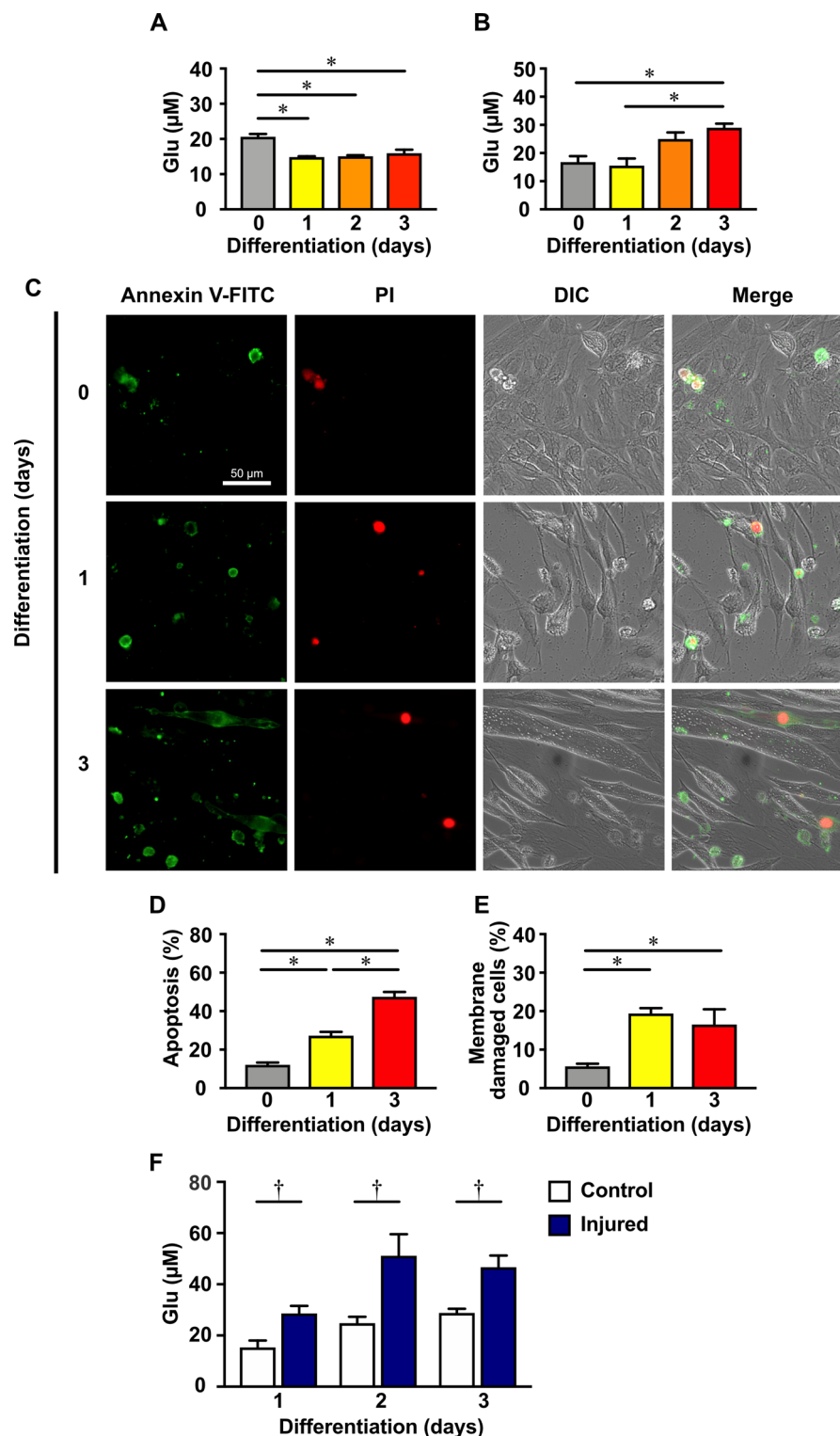


**Fig. 1.** Myocyte injury increases extracellular Glu. (A) The concentration of Glu in C2C12 cells was measured on days 0–3 of differentiation. (B) The concentration of Glu in the culture medium was measured on days 0–3 of C2C12 differentiation. (C) Apoptosis and membrane damage during C2C12 differentiation (days 0–3) were detected using Annexin V-FITC and PI. (D) The percentage of apoptotic cells was calculated from the cells within 360 μm × 270 μm area. (E) The percentage of annexin V-bound cells with plasma membrane-damage was calculated from all cells within 360 μm × 270 μm area using PI. (F) C2C12 cells on days 1–3 of differentiation were injured, and then the concentration of Glu in the culture medium was measured. As a control, the culture medium of intact cells was used. \* $P < 0.05$ , ANOVA with Tukey's multiple comparisons test,  $n = 3$ . † $P < 0.05$ , Student's t-test vs control,  $n = 3$ .

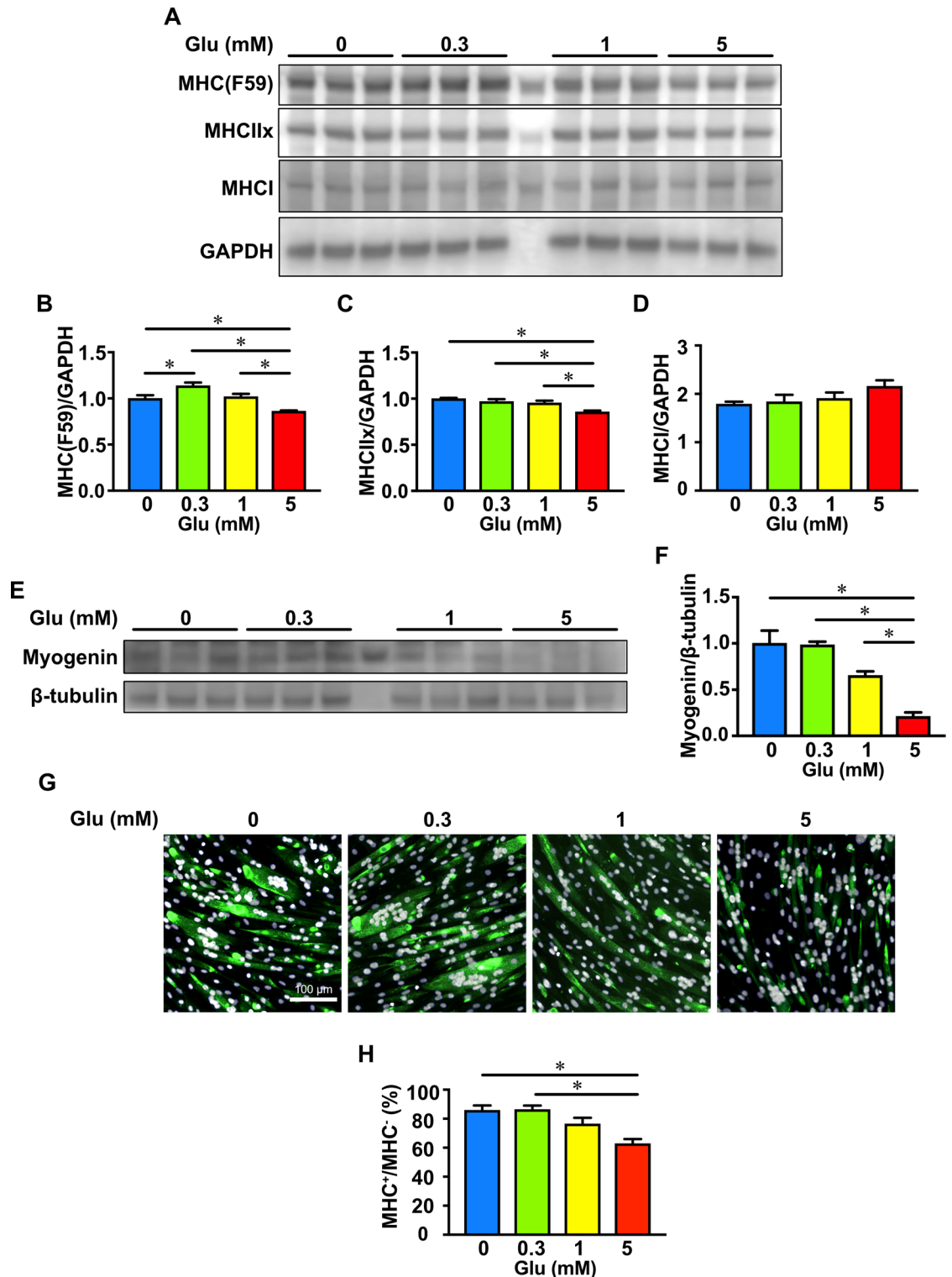


**Fig. 2.** High Glu concentrations suppresses the expression of fast-twitch myosin heavy chain (MHC) isoforms during the early stages of C2C12 differentiation. (A–F) C2C12 cells were differentiated in the presence of Glu (0, 0.3, 1, or 5 mM) for 2 days, and the expression levels of (B) MHC (F59), (C) MHCIIx, (D) MHCI, and (E,F) myogenin were analyzed using western blotting. GAPDH and  $\beta$ -tubulin were used as an internal standard. (G) C2C12 cells were differentiated for 3 days in the presence of Glu (0, 0.3, or 5 mM), followed by immunofluorescence using an anti-skeletal muscle myosin (F59) antibody (green). Nuclei were stained with DAPI (white). (H) The ratio of MHC (F59)-positive (MHC<sup>+</sup>) cells to MHC (F59)-negative (MHC<sup>-</sup>) cells was analyzed. The number of MHC<sup>+</sup> cells was determined by counting cells expressing MHC (F59), while MHC<sup>-</sup> cells were identified by counting DAPI-stained nuclei of cells lacking MHC (F59) expression. \* $P < 0.05$ , ANOVA with Tukey's multiple comparisons test,  $n = 3$ .



labeled via immunofluorescence using an anti-skeletal muscle myosin (F59) antibody (Fig. 3A). Cell phenotype and nuclear counts were analyzed to assess myocyte fusion. MHC<sup>+</sup> cells with three or more nuclei were defined as fused cells. Stimulation of C2C12 cells with 5 mM Glu increased the percentage of mononuclear cells and decreased that of fused cells (Fig. 3A,B). Furthermore, myotube area and width decreased (Fig. 3A,C,D). When the early stages of C2C12 differentiation is suppressed, the start of cell fusion, which follows the increase in MHC expression, is delayed. This implies a delay from the onset of differentiation to fusion. To determine whether high concentrations Glu stimulation directly affects the C2C12 fusion process, C2C12 cells on day 3 of differentiation, when fast-twitch MHC expression levels plateau (Fig. S5), were stimulated with 5 mM Glu for 2 days. The

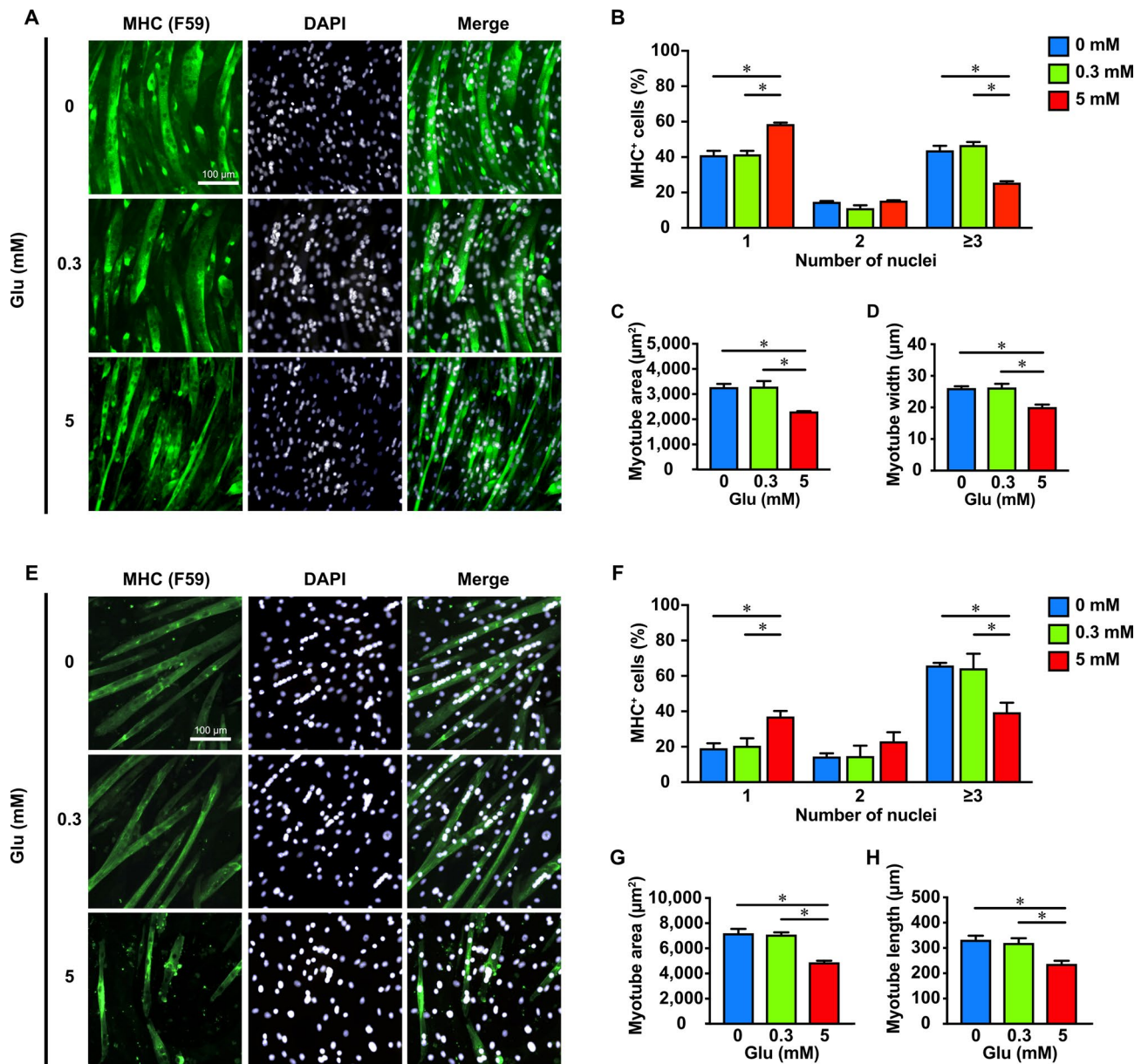


**Fig. 3.** High Glu concentration inhibits C2C12 cell fusion. (A) C2C12 cells were differentiated for 3 days in the presence of Glu (0, 0.3, or 5 mM), followed by immunofluorescence using anti-MHC (F59) antibody. Nuclei were stained with DAPI. (B) MHC (F59)-positive (MHC<sup>+</sup>) cells were classified by the number of nuclei as 1, 2, or ≥3. (C) The surface area and (D) width were measured in MHC<sup>+</sup> cells with 3 or more nuclei. (E) C2C12 cells were first differentiated for 3 days without the addition of Glu, then further induced to differentiate for an additional 2 days in the presence of Glu at concentrations of 0, 0.3, 1, or 5 mM. Following Glu stimulation, immunofluorescence was performed using the anti-MHC (F59) antibody. Nuclei were stained with DAPI. (F) MHC<sup>+</sup> cells were classified by the number of nuclei as 1, 2, or ≥3. (G) The surface area and (H) length were measured in MHC<sup>+</sup> cells with 3 or more nuclei. \**P* < 0.05, ANOVA with Tukey's multiple comparisons test, *n* = 3.

increase in cell surface area, length, and fused cells during the C2C12 fusion process was suppressed compared to control (Fig. 3E–H).

### High Glu concentration reduces the expression of mGluR5 and NMDAR in C2C12 cells

In skeletal muscle cells, mGluR5 and NMDAR are predominantly expressed as glutamate receptors<sup>9,10</sup>. C2C12 cells were induced to differentiate for 2 days in the presence of 0–5 mM Glu, after which the plasma membrane fraction was extracted (Fig. S6). When C2C12 cells were stimulated with 5 mM Glu, the expression level of mGluR5 on the plasma membrane was reduced compared to stimulation with 0.3 mM Glu (Figs. 4A,B and S7). Similarly, mGluR5 expression was reduced in whole cells (Figs. 4C,D and S8). The expression levels of NMDAR on the plasma membrane and in the whole cell also decreased by stimulation with 5 mM Glu (Figs. 4E–H, S9, and S10). Additionally, stimulation with 5 mM Glu for 2 days, starting on day 3 of C2C12 differentiation, reduced the expression levels of mGluR5 and NMDAR in whole cells (Figs. 4I–K and S11). These results indicate that high concentrations of Glu reduce the expression of Glu receptors, regardless of the timing of stimulation.

### mGluR5 and NMDAR play crucial roles in the regulation of the early stages of C2C12 differentiation

The correlation between mGluR5 and NMDAR activity and the early stages of C2C12 differentiation was examined using agonists and antagonists of these receptors. When C2C12 cells were stimulated with 30  $\mu$ M RO 4956371 (CTEP), a negative allosteric modulator of mGluR5 with inverse agonist properties<sup>23</sup>, the expression level of MHCIIx decreased significantly on day 2 of differentiation (Figs. 5A and S12). On day 3 of differentiation, the percentage of mononuclear myocytes increased, whereas that of the fused cells decreased (Fig. 5B,C). The surface area and width of the C2C12 cells decreased in a concentration-dependent manner (Fig. 5B,D,E). When

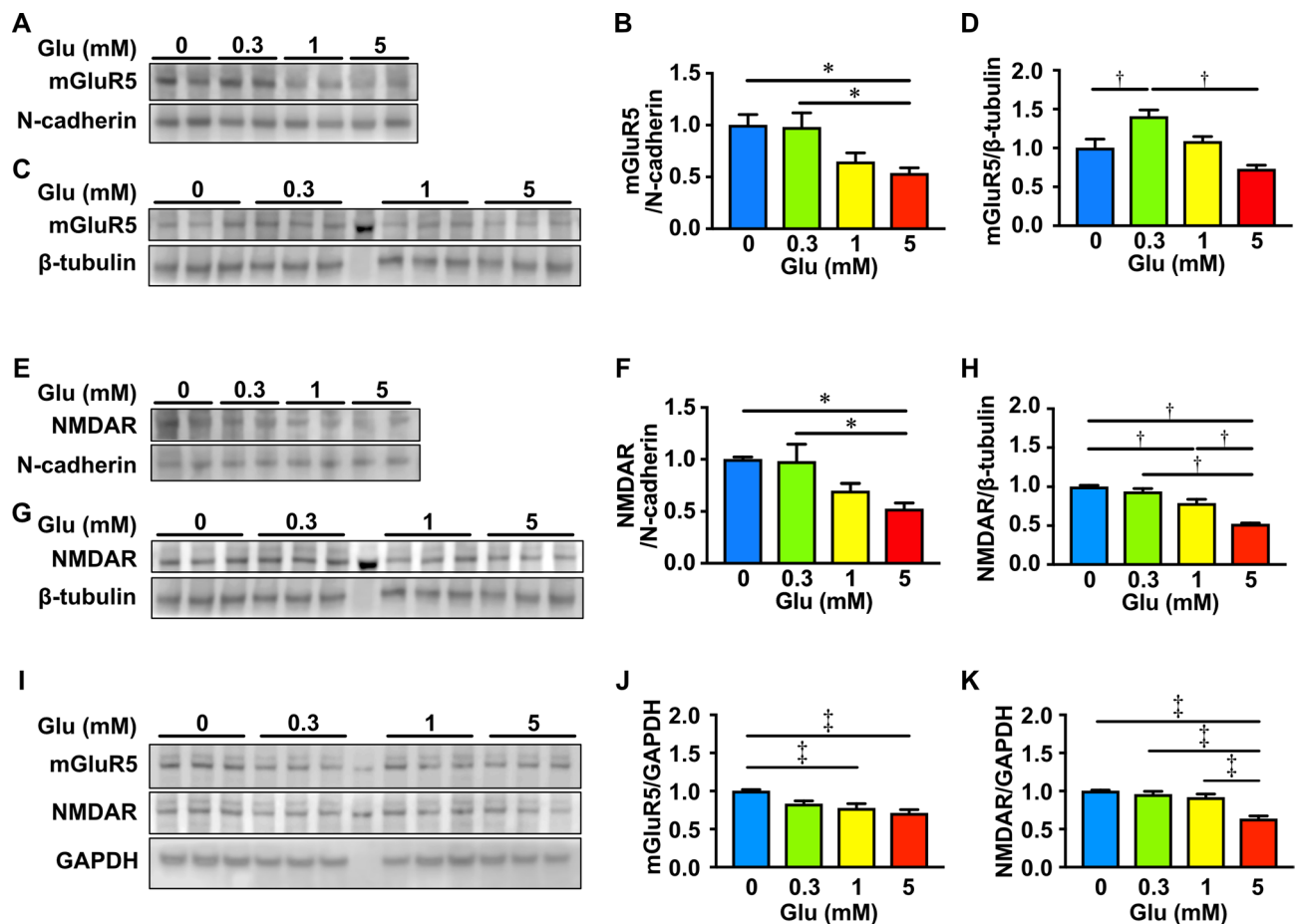


**Fig. 4.** High Glu concentration reduces the expression of mGluR5 and NMDAR in C2C12 cells. (A–H) C2C12 cells were differentiated in the presence of Glu (0, 0.3, 1, or 5 mM) for 2 days, followed by analyzing mGluR5 expression at (A,B) the plasma membrane and in (C,D) whole cells using western blotting. NMDAR expression at (E,F) the plasma membrane and in (G,H) whole cells. N-cadherin or GAPDH was served as the internal standard. (I–K) After C2C12 cells were differentiated for 3 days, they were further differentiated for 2 days in the presence of Glu (0, 0.3, 1, or 5 mM). The expression of (J) mGluR5 and (K) NMDAR in whole cells was analyzed using western blotting. \* $P < 0.05$ , ANOVA with Tukey's multiple comparisons test,  $n = 5$ . † $P < 0.05$ , ANOVA with Tukey's multiple comparisons test,  $n = 3$ . ‡ $P < 0.05$ , ANOVA with Tukey's multiple comparisons test,  $n = 6$ .

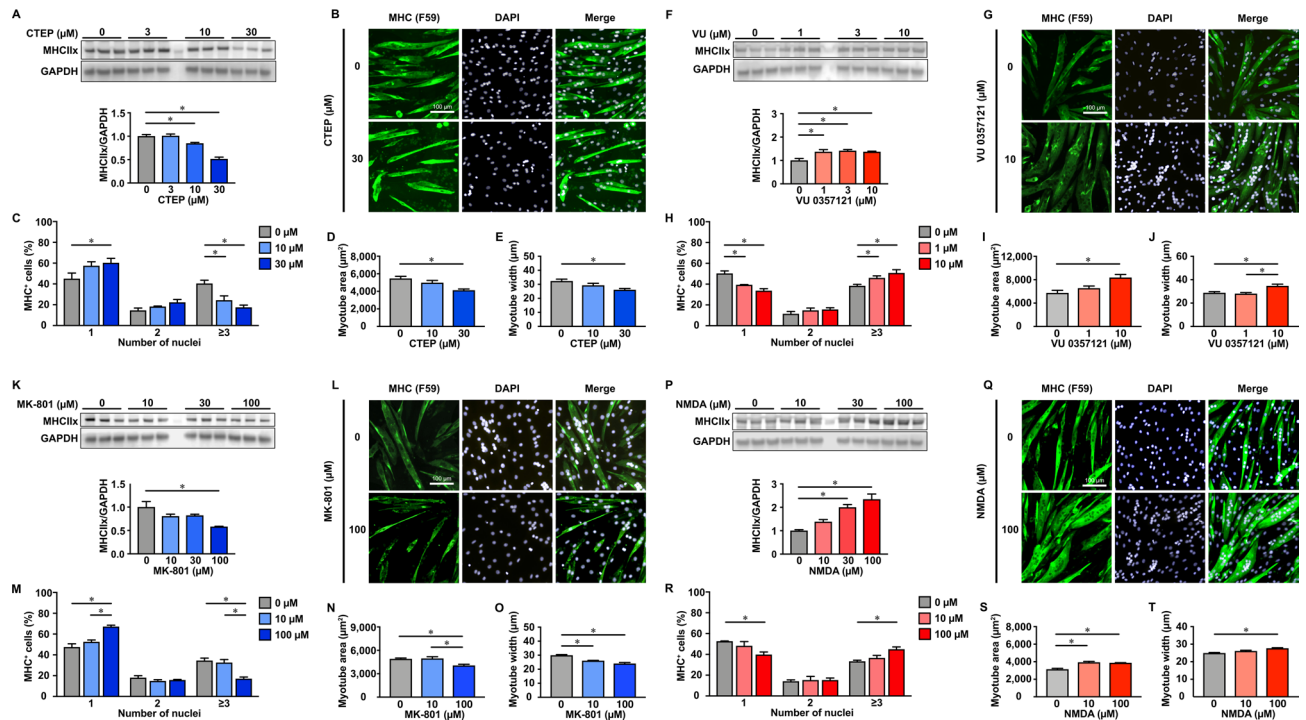


**Fig. 5.** mGluR5 and NMDAR play crucial roles in the regulation of the early stages of C2C12 differentiation. **(A)** C2C12 cells were differentiated in the presence of mGluR5 inhibitor CTEP for 2 days, and then the expression level of MHCIIx was analyzed using western blotting. GAPDH was used as an internal standard. **(B)** Cells were differentiated in the presence of CTEP for 3 days, followed by immunofluorescence using the anti-MHC (F59) antibody. Nuclei were stained with DAPI. **(C)** MHC (F59)-positive (MHC<sup>+</sup>) cells were classified by the number of nuclei as 1, 2, or  $\geq 3$ . **(D)** The surface area and **(E)** width were measured in MHC<sup>+</sup> cells with  $\geq 3$  nuclei. **(F)** Cells were differentiated in the presence of mGluR5 agonist VU 0357121 for 2 days, and then the expression level of MHCIIx was analyzed. **(G,H)** Cells were differentiated in the presence of VU 0357121 for 3 days, followed by immunofluorescence and nuclear classification. **(I)** The surface area and **(J)** width were measured in MHC<sup>+</sup> cells with  $\geq 3$  nuclei. **(K)** Cells were differentiated in the presence of NMDAR inhibitor MK-801 for 2 days, and then the expression level of MHCIIx was analyzed. **(L,M)** Cells were differentiated in the presence of MK-801 for 3 days, followed by immunofluorescence and nuclear classification. **(N)** The surface area and **(O)** width were measured in MHC<sup>+</sup> cells with  $\geq 3$  nuclei. **(P)** Cells were differentiated in the presence of NMDA for 2 days, and then the expression level of MHCIIx was analyzed. **(Q,R)** Cells were differentiated in the presence of NMDA for 3 days, followed by immunofluorescence and nuclear classification. **(S)** The surface area and **(T)** width were measured in MHC<sup>+</sup> cells with  $\geq 3$  nuclei. \* $P < 0.05$ , ANOVA with Tukey's multiple comparisons test,  $n = 3$ .

C2C12 cells were treated with 5 mM Glu and CTEP simultaneously during differentiation into myocytes, the expression levels of MHCIIx were reduced compared to treatment with 5 mM Glu alone (Fig. S13A). In addition, C2C12 cell fusion, as well as myocyte surface area and width, were also suppressed (Fig. S13B–E). In contrast, stimulation of C2C12 cells at the start of differentiation using 10  $\mu$ M VU 0357121, an allosteric activator of mGluR5<sup>24</sup>, increased MHCIIx expression levels on day 2 of differentiation (Figs. 5F and S14). On day 3, the percentage of mononuclear myocytes decreased, whereas that of the fused cells increased (Fig. 5G,H). Furthermore, both the surface area and width of myocytes increased in the presence of the activator (Fig. 5G,I,J). When C2C12 cells were differentiated in the presence of 100  $\mu$ M (+)-dizocilpine maleate (MK-801), an open-channel NMDAR blocker<sup>25</sup>, the expression level of MHCIIx decreased on day 2 of differentiation (Figs. 5K and S15). The percentage of mononuclear myocytes increased, and the percentage of fused cells decreased on day 3 (Fig. 5L,M). Both the surface area and the width of the cells were reduced significantly (Fig. 5L,N,O). Stimulation with 5 mM Glu and MK-801 simultaneously during the induction of C2C12 differentiation did not enhance the inhibitory effect of 5 mM Glu on myogenesis (Fig. S13F–J). When C2C12 cells were stimulated with 100  $\mu$ M NMDA, the expression of MHCIIx increased in an NMDA concentration-dependent manner on day 2 of differentiation (Figs. 5P and S16). Furthermore, on day 3, the percentage of fused myocytes, as well as the cell surface area and width, increased (Fig. 5Q–T).

### High Glu concentration inhibits downstream signaling of Glu receptors during the early stages of C2C12 differentiation

In skeletal muscle, mGluR5 promotes glucose uptake<sup>9</sup>. Optimal glucose uptake is necessary to stimulate skeletal muscle differentiation<sup>26</sup>. In contrast, NMDAR regulates myocyte fusion by inducing Ca<sup>2+</sup> influx<sup>11</sup>. While both

mGluR5 and NMDAR are likely to play important roles in skeletal myogenesis, their underlying mechanisms remain poorly understood. As mentioned above, the expression of MHCIIx and myogenin, which primarily function in skeletal muscle, was reduced by stimulation with 5 mM Glu in C2C12 cells during the early stages of differentiation (Figs. 2A,C,E,F, S3, and S4). Therefore, we investigated the expression and activity of proteins thought to be involved in regulating MHCIIx and myogenin expression. The transcriptional coactivator peroxisome proliferator-activated receptor gamma coactivator 1-alpha (PGC-1 $\alpha$ ), the transcription factors myocyte enhancer factor 2A (MEF2A) and cAMP response element-binding protein (CREB) are known as key regulators of these proteins' expression. The expression level of PGC-1 $\alpha$  on day 2 of differentiation was reduced by stimulation with 5 mM Glu compared to 0 mM Glu (control) (Figs. 6A and S17). MEF2A phosphorylation at Thr312 decreased in a Glu concentration-dependent manner (Figs. 6B and S18). The phosphorylation at Thr180 and Tyr182 of p38 mitogen-activated protein kinase (p38MAPK), which regulates MEF2A activity<sup>27,28</sup>, was decreased (Figs. 6C and S19). CREB is activated by phosphorylation at Ser133<sup>29</sup>. The 5 mM Glu stimulation also reduced the phosphorylation level at Ser133 compared to control (Figs. 6D and S20). As shown in Fig. 4, a high level of Glu stimulation is thought to downregulate mGluR5 and NMDAR. This downregulation may decrease downstream signaling of these Glu receptors, which in turn may lead to reduced expression of MHCIIx and myogenin.

### mGluR5 and NMDAR expression in the TA muscles is reduced with age

In C2C12 cells, mGluR5 and NMDAR regulate the expression of fast-twitch MHCIIx (Fig. 5). In the fast-twitch TA muscle of C57BL/6 mice<sup>30</sup>, the expression of these receptors decreased with age, showing a significant decline at 64 weeks of age compared to 12 and 48 weeks (Figs. 7A,B, S21, and S22). In addition, the muscle weight also decreased at 64 weeks of age (Fig. 7C).

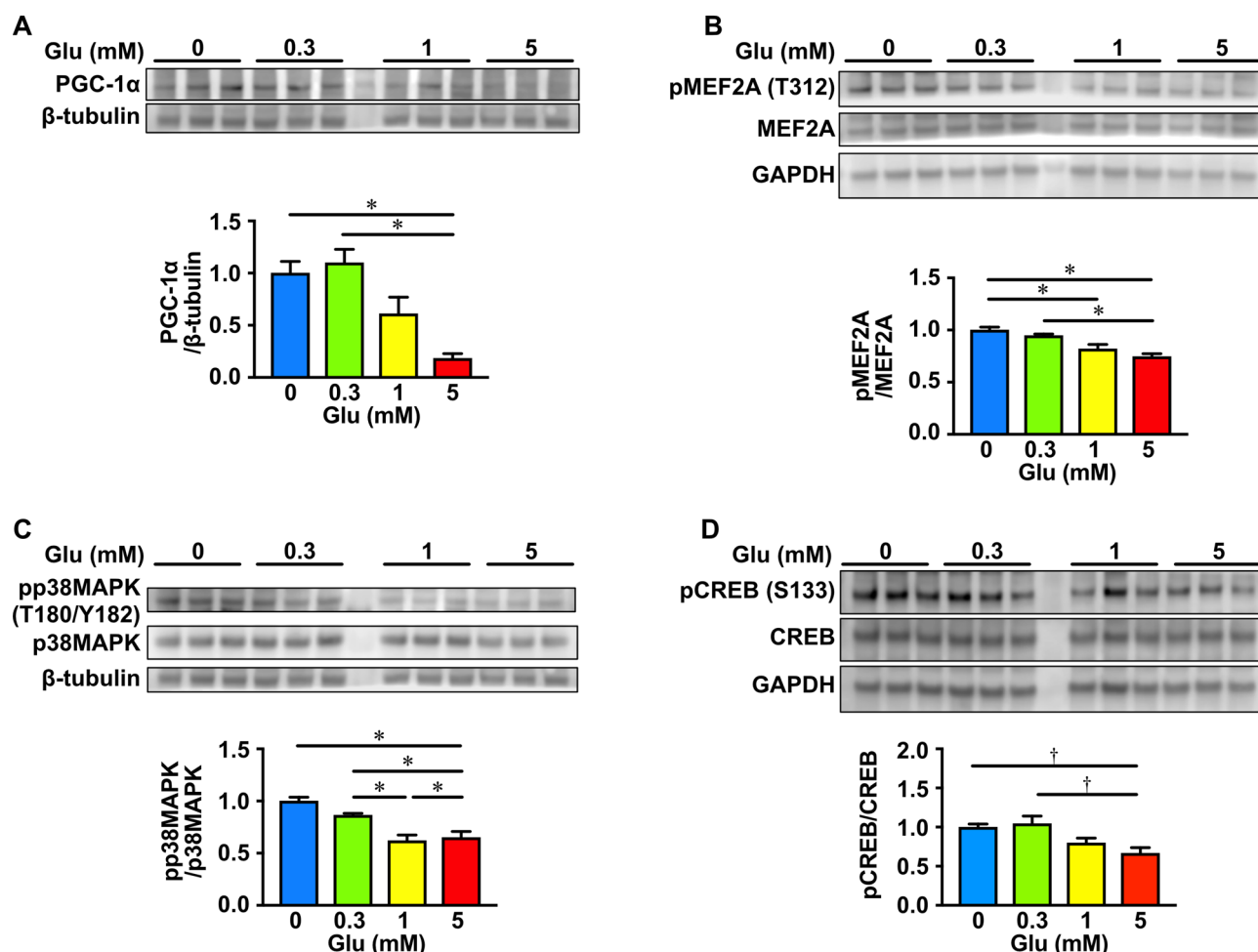


**Fig. 6.** High Glu concentration inhibits downstream signaling of Glu receptors during the early stages of C2C12 differentiation. C2C12 cells were differentiated for 2 days in the presence of Glu (0, 0.3, 1, or 5 mM), (A) PGC-1 $\alpha$ / $\beta$ -tubulin, (B) pMEF2A(T312)/MEF2A, (C) pp38MAPK (T180/Y182)/p38MAPK, (D) pCREB (S133)/CREB were analyzed using western blotting. \* $P$  < 0.05, ANOVA with Tukey's multiple comparisons test,  $n$  = 3. † $P$  < 0.05, ANOVA with Tukey's multiple comparisons test,  $n$  = 6.



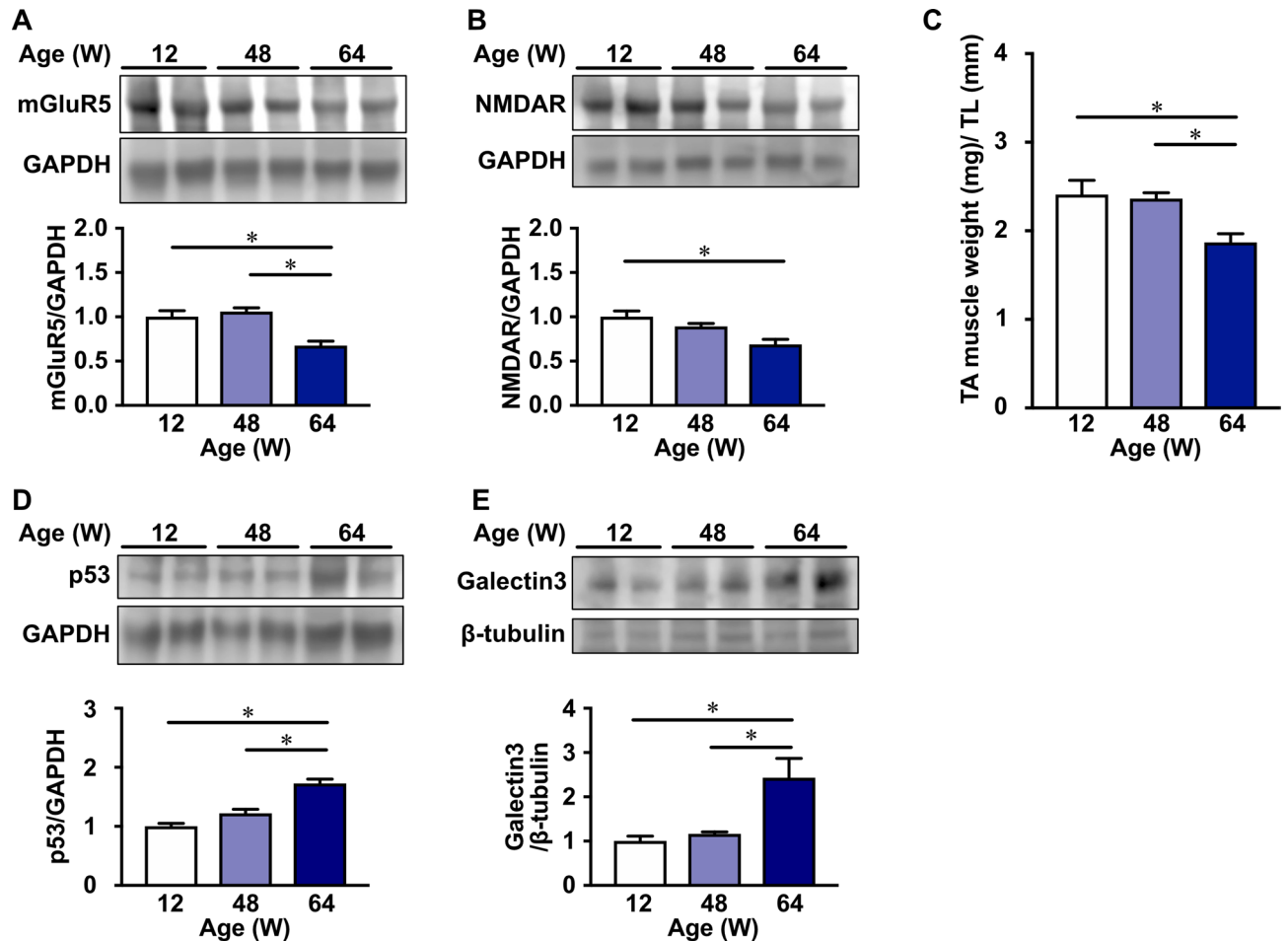


**Fig. 7.** mGluR5 and NMDAR expression in the tibialis anterior (TA) muscles is reduced with age. The expression levels of (A) mGluR5 and (B) NMDAR in the TA muscles were assessed via western blotting in mice aged 12–64 weeks. (C) The TA muscle weights of mice aged 12–64 weeks were measured and corrected by tibial length (TL). The aging markers (D) p53 and (E) galectin3 in TA muscles were analyzed by western blotting in mice 12–64 weeks of age.  $\beta$ -Tubulin or GAPDH served as the internal standard. \* $P < 0.05$ , ANOVA with Tukey's multiple comparisons test,  $n = 3$ –4.

## Discussion

Glu is abundant in myocytes, and when these cells are damaged during eccentric exercise or other activities, it can leak out and expose adjacent cells to high concentrations. In the present study, stimulation of C2C12 cells with a high concentration of Glu reduced the mGluR5 and NMDAR expression levels. In addition, the expression of muscle differentiation markers such as MHCIIx and myogenin, and cell fusion were also suppressed. In the TA muscles of late middle-aged mice, these Glu receptor levels and the muscle weight were reduced. These results suggest that reduced Glu receptor expression in myocytes inhibits skeletal myogenesis.

Caspase-3-mediated apoptosis is an essential factor for initiating differentiation in C2C12 cells<sup>31</sup>. If apoptotic cells are not efficiently removed by phagocytes, apoptosis may progress to secondary necrosis, which is accompanied by plasma membrane damage<sup>32</sup>. We observed an increase in the percentage of cells undergoing apoptosis and exhibiting membrane damage during the differentiation of C2C12 cells (Fig. 1C–E), suggesting leakage of intracellular Glu. In fact, Glu concentration in cell culture medium increased from day 2 of differentiation (Fig. 1B). On day 1 of differentiation, despite a decrease in overall cellular Glu (Fig. 1A), there was little increase in extracellular Glu (Fig. 1B). Glu was quantified after cells were washed with PBS and lysed in lysis buffer, a process which removes Glu from cells with damaged plasma membranes, resulting in a decrease in overall cellular Glu content. If Glu had been released immediately from cells with damaged plasma membranes, the extracellular Glu concentration would have increased at an earlier stage. However, since the damaged cells stained with PI did not rupture and retained their structural integrity, the release of intracellular Glu into the extracellular fluid was likely slower. Therefore, it can be considered that there was little increase in extracellular Glu on day 1 of differentiation. Leakage of cell contents due to membrane damage can affect surrounding cells, potentially causing inflammatory reactions<sup>33</sup>. When skeletal muscle is injured during eccentric exercise, plasma membrane damage occurs, exposing the surrounding myocytes to high concentrations of Glu due to the leakage of intracellular Glu. We confirmed that physical injury to C2C12 cells increased the extracellular

Glu concentration (Fig. 1F). However, in the cell culture protocol used in this study, the large volume of culture medium limited the Glu concentration to a maximum of ~30  $\mu$ M (Fig. 1B). The impact of leaked Glu on intact cells is expected to be minimal, as stimulation of C2C12 cells with 0.3 mM Glu had little effect on myotube formation (Fig. 2). In vivo, the volume of extracellular fluid surrounding the cells is much smaller. Therefore, developing a method to culture cells with reduced fluid volume would allow the effects of Glu to be studied under conditions more closely resembling those in vivo. Furthermore, Glu leaked from the cells is likely to be rapidly cleared into the bloodstream. Gutierrez et al. inserted microdialysis probes into human skeletal muscle tissue to measure amino acid concentrations in the extracellular fluid<sup>34</sup>. They observed that immediately after probe insertion, amino acids with high intracellular concentrations, including Glu, leaked from the cells, leading to increased extracellular concentrations. After more than 150 min, the extracellular Glu concentration decreased to levels comparable to those in the blood. This suggests that cells near the injured site might be exposed to leaked Glu for a few hours. In the present study, we examined the effects of high Glu concentrations in C2C12 cells. However, to fully understand the effects of Glu on actual muscle tissue, mature myocytes, satellite cells, and non-muscle cells must also be considered. Further studies are required to fully elucidate the dynamics of Glu leakage from muscle cells in vivo.

In humans, Glu concentrations in the plasma are usually around 0.1–0.3 mM, maintaining homeostasis<sup>35,36</sup>. Approximately 95% of the food-derived Glu taken up by the intestine is utilized by intestinal mucosal cells, and nearly 90% of the absorbed Glu is used by the liver<sup>37</sup>. Therefore, only a small fraction of diet-derived Glu is transferred to the bloodstream. In the present study, stimulation of C2C12 cells with 0.3 mM Glu, a concentration close to the physiological blood level, neither promoted nor inhibited skeletal myogenesis (Figs. 2 and 3). As shown in Fig. 1B, at least ~30  $\mu$ M Glu is present in the extracellular fluid during C2C12 differentiation, even in the absence of exogenous Glu. Establishing a method to differentiate C2C12 cells into myocytes while preventing intracellular Glu leakage could help clarify the effects of lower Glu concentrations on myogenesis.

mGluR5 is a Gq-coupled receptor that increases intracellular  $\text{Ca}^{2+}$  through the phospholipase C (PLC)/inositol 1,4,5-trisphosphate ( $\text{IP}_3$ ) signaling pathway. NMDAR increase intracellular  $\text{Ca}^{2+}$  by mediating  $\text{Ca}^{2+}$  influx from the extracellular fluid. The intracellular  $\text{Ca}^{2+}$  activates the  $\text{Ca}^{2+}$ -binding protein calpain, which subsequently activates p38 MAPK<sup>38</sup>. p38MAPK phosphorylates transcription factors MEF2A and increases its activity<sup>28</sup>. MEF2A enhances gene expression of proteins required for myogenesis, such as PGC-1 $\alpha$  and myogenin<sup>39,40</sup>. PGC-1 $\alpha$  gene expression is also upregulated by CREB<sup>41</sup>. PGC-1 $\alpha$  promotes skeletal myogenesis by stimulating MHCIIx gene expression<sup>42</sup>. A high concentration of Glu (5 mM) decreased MHCIIx and myogenin expression through suppression of these signaling cascades (Figs. 2A,C,E,F and 6). In addition, 5 mM Glu reduced the expression of mGluR5 and NMDAR on the plasma membrane (Fig. 4A,B,E,F). mGluR5 activates protein kinase C (PKC) through PLC/diacylglycerol (DAG) pathway. Activated PKC phosphorylates mGluR5 and reduces its cell surface expression<sup>43</sup>. Furthermore, mGluR5 activation is accompanied by a decrease in the surface expression of NMDA receptors at the plasma membrane<sup>44</sup>. Therefore, exposure to 5 mM Glu may result in the downregulation of Glu receptors and suppression of their downstream signaling pathways, thereby reducing the expression levels of MHCIIx and myogenin required for C2C12 differentiation into skeletal muscle. In the present study, the mechanisms by which the signaling upstream of p38 MAPK, particularly  $\text{Ca}^{2+}$ -mediated signaling, was altered in response to high levels of Glu stimulation could not be fully elucidated. Future research will address this.

Stimulation of C2C12 cells with 5 mM Glu during the early stages of differentiation reduced myocyte fusion (Fig. 3A–D). This decrease was accompanied by reduced expression of mGluR5 and NMDAR, suggesting that downregulation of these Glu receptors led to suppressed MHCIIx and myogenin expression, thereby delaying the subsequent fusion process (Figs. 2A,C,E,F and 4A–H). Expression levels of fast-twitch MHC (F59) and MHCIIx alone, increased until day 3 of differentiation and remained stable through day 7 (Fig. S5). In the later stages of differentiation, after the third day of differentiation induction, high Glu concentrations similarly reduced Glu receptor expression and decreased myocyte fusion (Figs. 3E–H and 4I–K). This indicates that high Glu concentrations suppress cell fusion itself via Glu receptors.

Suppression of MHCIIx expression levels and myocyte fusion was observed not only with 5 mM Glu but also with CTEP and MK-801 (Fig. 5A–E,K–O). When C2C12 cells were simultaneously treated with 5 mM Glu and these Glu receptor inhibitors, CTEP further suppressed myogenesis already inhibited by 5 mM Glu, whereas MK-801 did not (Fig. S13). This suggests that mGluR5-mediated signaling may play a greater role in myogenesis than NMDAR-mediated intracellular signaling. However, not only mGluR5 agonists, but also NMDAR agonists, increased MHCIIx expression levels in C2C12 and promoted myocyte fusion (Fig. 5F–J,P–T). It is suggested that both glutamate receptors regulate C2C12 cell differentiation, but further studies are needed to fully understand the mechanisms.

When glucose is taken up by the myocytes, glycolysis is activated, and ATP is subsequently produced in the mitochondria. Intracellular Glu is converted into  $\alpha$ -ketoglutarate, an intermediate in the TCA cycle, which facilitates ATP production. Impairment of mitochondrial function and activity is thought to inhibit myogenesis<sup>45</sup>. Loss of glucose uptake not only reduces cell viability, but also inhibits myogenesis<sup>46</sup>. Thus, intracellular Glu could play an important role in myogenesis. Meanwhile, cytoplasmic concentrations of Glu in human primary myotubes are extremely high and are barely affected by changes in extracellular Glu concentrations, due to low levels of transporter-mediated Glu transport<sup>7</sup>. Therefore, it was suggested that high extracellular Glu concentrations may regulate myogenesis through Glu receptors.

In humans, with aging, the composition of phospholipids, such as phosphatidylcholine and phosphatidylethanolamine, changes due to an increase in fatty acid-binding protein 3 expression, making the plasma membrane more fragile<sup>47</sup>. Additionally, the age-related decrease in collagen and elastin, which are components of the extracellular matrix, contributes to plasma membrane fragility<sup>48</sup>. As a result, skeletal muscle cells may become more susceptible to damaging stimuli, such as eccentric exercise, during aging, leading to increased Glu leakage. Exercise can cause up to a 100-fold increase in blood flow to skeletal muscle compared to

resting conditions<sup>49</sup>. Therefore, in healthy individuals, Glu leaked during strenuous exercise is likely to be rapidly transported into the bloodstream and subsequently excreted by the kidneys<sup>50</sup>. However, in the elderly, impaired microcirculation and other factors slow blood flow<sup>51,52</sup>, which may delay Glu clearance and prolong muscle cell exposure to high Glu levels.

In C2C12 cells, high Glu concentrations decreased the expression of mGluR5 and NMDAR, resulting in decreased expression of several fast-twitch MHC isoforms, including MHCIIX, while the expression of slow-twitch MHCI remained unchanged (Figs. 2A–D and 4). These results suggest that high concentrations of Glu inhibit primarily fast-twitch muscle maturation through downregulation of Glu receptors. When the expression levels of mGluR5 and NMDAR in the TA muscles of C57BL/6 mice were examined at 12, 48, and 64 weeks of age, a decrease was observed at 64 weeks (Fig. 7A,B). In the mice, 48 and 64 weeks of age are considered middle-aged<sup>53</sup>, but significant increases in aging markers such as p53 and galectin3<sup>54,55</sup> were observed at 64 weeks, indicating late middle age (Figs. 7D,E, S23, and S24). In addition, we confirmed that the weight of the TA muscles decreased at 64 weeks of age (Fig. 7C). In humans, the mass of the TA muscles decreases with aging<sup>56</sup>. This study suggests that age-related loss of TA muscle is associated with decreased expression of Glu receptors. Further studies are planned to clarify the relationship between this phenomenon and elevated extracellular Glu concentrations.

## Materials and methods

### Materials

Anti-MYH1 (1:500, Cat# ZRB1214), anti-MYH7 (1:500, Cat# MABT838), anti-PGC-1 $\alpha$  (1:500, Cat# KP9803), anti-mGluR5 (1:500, Cat# MABN540), anti-NMDAR (1:500, Cat# 5704S), anti-rabbit IgG (1:5000, Cat# A0545) and anti-mouse IgG (1:5000, Cat# A4416) were purchased from Merck (Darmstadt, Germany). Anti-Skeletal Muscle Myosin (F59) (1:500, Cat# sc-32732) was from Santa Cruz Biotechnology (Dallas, TX, USA). Anti-p38MAPK (T180/Y182) (1:500, Cat# 9216S), anti-p38MAPK (1:500, Cat# 8690S), anti-pCREB (S133) (1:500, Cat# 9198S), anti-CREB (1:500, Cat# 9104S), anti- $\beta$ -tubulin (1:500, Cat# 2128S), anti-N-cadherin (1:500, Cat# 14215S) and anti-p53 (1:500, Cat# 2524S) were from Cell signaling technology (Beverly, MA, USA). Anti-pMEF2A (T312) (1:500, Cat# ab30644), anti-Myogenin (1:500, Cat# ab1835), anti-MEF2A (1:500, Cat# ab181494) and anti-galectin3 (1:500, Cat# ab2785) were from Abcam (Cambridge, UK). Anti-GAPDH (1:500, Cat# M171-3) was from MBL Life Science (Tokyo, Japan). L-glutamic acid (Cat# 070-00502) was from Wako pure chemical industries (Osaka, Japan). RO4956371 (CTEP) (Cat# S2861), VU 0357121 (Cat# S279501) and NMDA (*N*-Methyl-D-aspartic acid) (Cat# S7072) were from Selleck Chemicals (Houston, TX, USA). (+)-MK 801 Maleate (Cat# 130-17381) was from Fujifilm (Osaka, Japan). The dilution ratio in each antibody was for western blotting.

### Cell culture

To investigate the effect of Glu on skeletal myogenesis, C2C12 mouse-derived skeletal muscle cells (Greiner Bio-One, Kremsmünster, Austria) with the ability to differentiate from myoblasts into myotubes were used. The cells were cultured at 37 °C with 5% CO<sub>2</sub> in growth medium consisting of 4.5 g/L D-glucose-containing, Glu-free Dulbecco's modified eagle's medium (DMEM) supplemented with 1% penicillin–streptomycin (PS) and 10% fetal bovine serum. Upon reaching 90% confluence, the medium was switched to differentiation medium consisting of DMEM supplemented with 1% PS and 2% horse serum, and the cells were cultured for 2–5 days.

### Glutamate assay

Glu concentrations in C2C12 cells and culture medium on days 0–3 of differentiation were measured using the Glutamate Assay Kit-WST (Dojindo laboratories, Kumamoto, Japan) according to the manufacturer's protocol. Briefly, to measure intracellular Glu concentrations, the C2C12 lysates (final volume of 200  $\mu$ L) were incubated with a working solution at 37 °C for 30 min. After incubation, the absorbance was measured at 450 nm using plate reader (Spectramax<sup>®</sup> i3, Molecular devices Ltd, Sunnyvale, CA, USA). Similarly, the concentration of Glu in the culture medium was measured. To determine the concentration of leaked Glu due to cell injury, the culture medium was first replaced with serum-free DMEM with 1% PS, and the cells were incubated at 37 °C for 5 h. Then, the cells were physically stimulated with the pipette tip, and the concentration of Glu in the culture medium was measured. Physical stimulation was performed using a 12-channel micropipette to ensure uniform stimulation of the cells.

### Extraction of plasma membrane fraction

C2C12 cells were differentiated for 2 days, and the plasma membrane fraction was extracted using the Pierce<sup>™</sup> cell surface protein isolation kit (Thermo fisher scientific, Waltham, MA, USA). Briefly, the cells were washed three times using PBS (–) and then incubated with Sulfo-NHS-SS-Biotin for 30 min at 4 °C. The reaction was quenched by quenching solution. The cells were lysed in Pierce<sup>™</sup> IP Lysis Buffer with protease & phosphatase inhibitor (Cat# 78442, Thermo fisher scientific) for 30 min at 4 °C. The lysate was incubated with Pierce<sup>™</sup> NeutrAvidin<sup>™</sup> Agarose for 1 h at room temperature. Biotin-avidin-agarose complexes were washed three times in Wash Buffer (Cat# 1859389, Thermo fisher scientific) containing protease and phosphatase inhibitor, and added TBS (–) with 0.5% TritonX-100 and protease and phosphatase inhibitor. Plasma membrane proteins were eluted in NuPAGE<sup>®</sup> LDS sample buffer (Cat# NP0007, Thermo fisher scientific) with 100 mM ( $\pm$ )-Dithiothreitol (DTT), and then analyzed by western blotting.

### Western blotting

C2C12 cells on day 2 of differentiation were lysed in TBS (–) buffer containing 1% TritonX-100 and protease and phosphatase inhibitor (lysis buffer). Total cellular lysates were diluted in NuPAGE<sup>®</sup> LDS sample buffer with

100 mM DTT, and incubated at 70 °C for 15 min. The protein samples were separated on a NuPAGE™ Bis-Tris Gel (Cat# NP0323BOX, Thermo fisher scientific) and transferred to a polyvinylidene difluoride (PVDF) membrane (cytiva, Tokyo, Japan), which was then blocked in Blocking One (Nacalai Tesque, Kyoto, Japan) for 1 h at room temperature. Next, the PVDF membrane was incubated with the primary antibodies for 1 h at room temperature. The membrane was washed by TBS with 0.1% Tween® 20, followed by a 1 h incubation at room temperature with horseradish peroxidase (HRP)-conjugated secondary antibodies. The antigen-antibody peroxidase complex was detected using Supersignal™ west femto maximum sensitivity substrate (Thermo fisher scientific), and the images were generated using c-DiGit® Blot scanner (LI-COR, Lincoln, NE, USA). The intensity of each band was determined by ImageJ/Fiji version 1.54. Protein expression of MHCIIx or MHC (F59) was used as an indicator of myoblasts to myocytes differentiation<sup>20</sup>.

### Immunofluorescence

C2C12 cells on day 3 of differentiation were fixed with Mildform®10NM (Fujifilm, Osaka, Japan), washed by PBS (–) containing 0.5% Triton X-100 for 10 min, and then blocked with Blocking One for 30 min at room temperature. The fixed cells were incubated for 1 h at room temperature with anti-MHC (F59) antibody (1:400), and for 1 h with Alexa Fluor™488 goat anti-rabbit IgG (1:500, Cat# A32723, Thermo fisher scientific). Fluorescent images were analyzed by BZ-X810 fluorescence microscopy (Keyence, Osaka, Japan). 4,6-Diamidino-2-phenylindole (DAPI) (Dojindo, Kumamoto, Japan) staining was performed to show the position of the nuclei. MHC (F59)-positive cells were classified based on the number of nuclei (one, two, or three or more) and marked differently. The number of each marker was counted as the number of cells. MHC (F59)-positive cells with three or more nuclei were evaluated as fusion cells<sup>57</sup>. Myocyte maturity was assessed by surface area, length and width of the cells<sup>58–60</sup>. These categories were analyzed using ImageJ/Fiji version 1.54.

### Detection of apoptosis and plasma membrane damage

Annexin V-FITC apoptosis detection kit (nacalai tesque) was used to detect Apoptosis and plasma membrane damage in C2C12 cells. Briefly, C2C12 cells reaching 90% confluence were incubated in differentiation medium for 0–3 days. The cells were washed twice with PBS (–) and then reacted with Annexin V-FITC and PI for 15 min in the dark. Annexin V detects the early stage of apoptosis by binding to phosphatidylserine exposed on the cell surface. PI is not membrane permeable, but when the plasma membrane is damaged, it binds to DNA in the nucleus and emits fluorescence, thus detecting membrane-damaged cells. Fluorescent images were analyzed using BZ-X810 fluorescence microscopy.

### Ethical declarations for conducting animal studies

All animal experiments were conducted in accordance with the ARRIVE guidelines and approved by the Institutional Animal Care and Use Committee of Showa University (Permit Number: 324044), in compliance with the Japanese Government's regulations for the care and use of laboratory animals.

### Isolation of the mouse TA muscles

C57BL/6 mice were purchased from Sankyo Laboratory (Tokyo, Japan). After the mice were euthanized via CO<sub>2</sub> inhalation, the TA muscles were excised, followed by the measurement of the muscle weight. Tibia length was used to adjust for muscle weight. The muscle tissue was then homogenized in lysis buffer to prepare western blotting samples.

### Statistical analysis

The results were expressed as the mean ± standard error. Statistical analysis was performed by the Student's t-test or one-way analysis of variance (ANOVA) with Tukey's multiple comparisons test using GraphPad Prism 7 (GraphPad Software, San Diego, CA, USA). A *P* value < 0.05 was interpreted as statistically significant.

### Data availability

Data supporting the findings of this study are available from the corresponding author upon reasonable request.

Received: 23 October 2024; Accepted: 8 May 2025

Published online: 19 May 2025

### References

- Hindi, S. M., Tajrishi, M. M. & Kumar, A. Signaling mechanisms in mammalian myoblast fusion. *Sci. Signal.* **6**, re2 (2013).
- Yin, H., Price, F. & Rudnicki, M. A. Satellite cells and the muscle stem cell niche. *Physiol. Rev.* **93**, 23–67 (2013).
- Tapiero, H., Mathé, G., Couvreur, P. & Tew, K. D. II. Glutamine and glutamate. *Biomed. Pharmacother.* **56**, 446–457 (2002).
- Brosnan, J. T. Glutamate, at the interface between amino acid and carbohydrate metabolism. *J. Nutr.* **130**, S988–S990 (2000).
- Meldrum, B. S. Glutamate as a neurotransmitter in the brain: Review of physiology and pathology. *J. Nutr.* **130**, S1075–S1015 (2000).
- Lau, A. & Tymianski, M. Glutamate receptors, neurotoxicity and neurodegeneration. *Pflugers Arch.* **460**, 525–542 (2010).
- Gauthier-Coles, G. et al. Quantitative modelling of amino acid transport and homeostasis in mammalian cells. *Nat. Commun.* **12**, 5282 (2021).
- Rutten, E. P., Engelen, M. P., Schols, A. M. & Deutz, N. E. Skeletal muscle glutamate metabolism in health and disease: State of the art. *Curr. Opin. Clin. Nutr. Metab. Care* **8**, 41–51 (2005).
- Kim, J. H. et al. The glutamate agonist homocysteine sulfinic acid stimulates glucose uptake through the calcium-dependent AMPK-p38 MAPK-protein kinase C zeta pathway in skeletal muscle cells. *J. Biol. Chem.* **286**, 7567–7576 (2011).
- Endo, Y. et al. Exercise-induced gene expression changes in skeletal muscle of old mice. *Genomics* **113**, 2965–2976 (2021).
- Lee, K. H., Park, J. Y. & Kim, K. NMDA receptor-mediated calcium influx plays an essential role in myoblast fusion. *FEBS Lett.* **578**, 47–52 (2004).



12. Lukasiewicz, P. D., Bligard, G. W. & DeBrecht, J. D. EAAT5 glutamate transporter-mediated inhibition in the vertebrate retina. *Front. Cell. Neurosci.* **15**, 662859 (2021).
13. Kanai, Y. & Hediger, M. A. Primary structure and functional characterization of a high-affinity glutamate transporter. *Nature* **360**, 467–471 (1992).
14. Björn-Yoshimoto, W. E. & Underhill, S. M. The importance of the excitatory amino acid transporter 3 (EAAT3). *Neurochem. Int.* **98**, 4–18 (2016).
15. Proske, U. & Morgan, D. L. Muscle damage from eccentric exercise: Mechanism, mechanical signs, adaptation and clinical applications. *J. Physiol.* **537**, 333–345 (2001).
16. Sousa-Victor, P. & Muñoz-Cánoves, P. Regenerative decline of stem cells in sarcopenia. *Mol. Asp. Med.* **50**, 109–117 (2016).
17. Bergström, J., Fürst, P., Norée, L. O. & Vinnars, E. Intracellular free amino acid concentration in human muscle tissue. *J. Appl. Physiol.* **36**, 693–697 (1974).
18. Wang, J. & Walsh, K. Resistance to apoptosis conferred by Cdk inhibitors during myocyte differentiation. *Science* **273**, 359–361 (1996).
19. Henderson, M. A., Gillon, S. & Al-Haddad, M. Organization and composition of body fluids. *Anaesth. Intensive Care Med.* **22**, 511–517 (2021).
20. Allen, D. L. & Unterman, T. G. Regulation of myostatin expression and myoblast differentiation by FoxO and SMAD transcription factors. *Am. J. Physiol. Cell Physiol.* **292**, C188–C199 (2007).
21. Andrés, V. & Walsh, K. Myogenin expression, cell cycle withdrawal, and phenotypic differentiation are temporally separable events that precede cell fusion upon myogenesis. *J. Cell Biol.* **132**, 657–666 (1996).
22. Ennion, S., Sant' Ana Pereira, J., Sargeant, A. J., Young, A. & Goldspink, G. Characterization of human skeletal muscle fibres according to the myosin heavy chains they express. *J. Muscle Res. Cell Motil.* **16**, 35–43 (1995).
23. Lindemann, L. et al. CTEP: A novel, potent, long-acting, and orally bioavailable metabotropic glutamate receptor 5 inhibitor. *J. Pharmacol. Exp. Ther.* **339**, 474–486 (2011).
24. Hammond, A. S. et al. Discovery of a novel chemical class of mGlu(5) allosteric ligands with distinct modes of pharmacology. *ACS Chem. Neurosci.* **1**, 702–716 (2010).
25. Song, X. et al. Mechanism of NMDA receptor channel block by MK-801 and memantine. *Nature* **556**, 515–519 (2018).
26. Luo, W., Ai, L., Wang, B. F. & Zhou, Y. High glucose inhibits myogenesis and induces insulin resistance by down-regulating AKT signaling. *Biomed. Pharmacother.* **120**, 109498 (2019).
27. Raingeaud, J. et al. Pro-inflammatory cytokines and environmental stress cause p38 mitogen-activated protein kinase activation by dual phosphorylation on tyrosine and threonine. *J. Biol. Chem.* **270**, 7420–7426 (1995).
28. Zhao, M. et al. Regulation of the MEF2 family of transcription factors by p38. *Mol. Cell. Biol.* **19**, 21–30 (1999).
29. Gonzalez, G. A. & Montminy, M. R. Cyclic AMP stimulates somatostatin gene transcription by phosphorylation of CREB at serine 133. *Cell* **59**, 675–680 (1989).
30. Dusterhöft, S., Yablonka-Reuveni, Z. & Pette, D. Characterization of myosin isoforms in satellite cell cultures from adult rat diaphragm, soleus and tibialis anterior muscles. *Differentiation* **45**, 185–191 (1990).
31. Fernando, P., Kelly, J. F., Balazsi, K., Slack, R. S. & Megeney, L. A. Caspase 3 activity is required for skeletal muscle differentiation. *Proc. Natl. Acad. Sci. U.S.A.* **99**, 11025–11030 (2002).
32. Rogers, C. et al. Cleavage of DFNA5 by caspase-3 during apoptosis mediates progression to secondary necrotic/pyroptotic cell death. *Nat. Commun.* **8**, 14128 (2017).
33. Proskuryakov, S. Y., Konoplyannikov, A. G. & Gabai, V. L. Necrosis: A specific form of programmed cell death. *Exp. Cell Res.* **283**, 1–16 (2003).
34. Gutierrez, A., Anderstam, B. & Alvestrand, A. Amino acid concentration in the interstitium of human skeletal muscle: A microdialysis study. *Eur. J. Clin. Invest.* **29**, 947–952 (1999).
35. Zlotnik, A. et al. The effects of estrogen and progesterone on blood glutamate levels: Evidence from changes of blood glutamate levels during the menstrual cycle in women. *Biol. Reprod.* **84**, 581–586 (2011).
36. Yeung, S. S. Y., Zhu, Z. L. Y., Kwok, T. & Woo, J. Serum amino acids patterns and 4-year sarcopenia risk in community-dwelling Chinese older adults. *Gerontology* **68**, 736–745 (2022).
37. Reeds, P. J., Burrin, D. G., Stoll, B. & Jahoor, F. Intestinal glutamate metabolism. *J. Nutr.* **130**, S978–S982 (2000).
38. Kook, S.-H. et al. Involvement of p38 MAPK-mediated signaling in the calpeptin-mediated suppression of myogenic differentiation and fusion in C2C12 cells. *Mol. Cell. Biochem.* **310**, 85–92 (2008).
39. Czubryt, M. P., McAnally, J., Fishman, G. I. & Olson, E. N. Regulation of peroxisome proliferator-activated receptor gamma coactivator 1 alpha (PGC-1 alpha) and mitochondrial function by MEF2 and HDAC5. *Proc. Natl. Acad. Sci. U.S.A.* **100**, 1711–1716 (2003).
40. Johanson, M. et al. Transcriptional activation of the myogenin gene by MEF2-mediated recruitment of myf5 is inhibited by adenovirus E1A protein. *Biochem. Biophys. Res. Commun.* **265**, 222–232 (1999).
41. Popov, D. V., Lysenko, E. A., Kuzmin, I. V., Vinogradova, V. & Grigoriev, A. I. Regulation of PGC-1α isoform expression in skeletal muscles. *Acta Nat.* **7**, 48–59 (2015).
42. Arany, Z. et al. The transcriptional coactivator PGC-1β drives the formation of oxidative type IIX fibers in skeletal muscle. *Cell Metab.* **5**, 35–46 (2007).
43. Lee, J. H. et al. Calmodulin dynamically regulates the trafficking of the metabotropic glutamate receptor mGluR5. *Proc. Natl. Acad. Sci. U.S.A.* **105**, 12575–12580 (2008).
44. Snyder, E. M. et al. Internalization of ionotropic glutamate receptors in response to mGluR activation. *Nat. Neurosci.* **4**, 1079–1085 (2001).
45. Wagatsuma, A. & Sakuma, K. Mitochondria as a potential regulator of myogenesis. *Sci. World J.* **2013**, 593267 (2013).
46. Jang, M., Scheffold, J., Röst, L. M., Cheon, H. & Bruheim, P. Serum-free cultures of C2C12 cells show different muscle phenotypes which can be estimated by metabolic profiling. *Sci. Rep.* **12**, 827 (2022).
47. Lee, S. M. et al. FABP3-mediated membrane lipid saturation alters fluidity and induces ER stress in skeletal muscle with aging. *Nat. Commun.* **11**, 5661 (2020).
48. Csapo, R., Gumpenberger, M. & Wessner, B. Skeletal muscle extracellular matrix—What do we know about its composition, regulation, and physiological roles? A narrative review. *Front. Physiol.* **11**, 253 (2020).
49. Andersen, P. & Saltin, B. Maximal perfusion of skeletal muscle in man. *J. Physiol.* **366**, 233–249 (1985).
50. Tizianello, A., De Ferrari, G., Garibotto, G., Gurreri, G. & Robaudo, C. Renal metabolism of amino acids and ammonia in subjects with normal renal function and in patients with chronic renal insufficiency. *J. Clin. Invest.* **65**, 1162–1173 (1980).
51. Ungvari, Z., Tarantini, S., Donato, A. J., Galvan, V. & Csiszar, A. Mechanisms of vascular aging. *Circ. Res.* **123**, 849–867 (2018).
52. Jackson, D. N., Moore, A. W. & Segal, S. S. Blunting of rapid onset vasodilatation and blood flow restriction in arterioles of exercising skeletal muscle with ageing in male mice. *J. Physiol.* **588**, 2269–2282 (2010).
53. DE, H. Life Span as a Biomarker. <https://www.jax.org/research-and-faculty/research-labs/the-harrison-lab/gerontology/life-span-as-a-biomarker> (2017).
54. Rufini, A., Tucci, P., Celardo, I. & Melino, G. Senescence and aging: The critical roles of p53. *Oncogene* **32**, 5129–5143 (2013).
55. Johmura, Y. et al. Senolysis by glutaminolysis inhibition ameliorates various age-associated disorders. *Science* **371**, 265–270 (2021).
56. Markworth, J. F. et al. Metabolipidomic profiling reveals an age-related deficiency of skeletal muscle pro-resolving mediators that contributes to maladaptive tissue remodeling. *Aging Cell* **20**, e13393 (2021).

57. Yue, J. et al. Continuous exposure to isoprenaline reduced myotube size by delaying myoblast differentiation and fusion through the NFAT-MEF2C signaling pathway. *Sci. Rep.* **13**, 436 (2023).
58. White, R. B., Biérinx, A. S., Gnocchi, V. F. & Zammit, P. S. Dynamics of muscle fibre growth during postnatal mouse development. *BMC Dev. Biol.* **10**, 21 (2010).
59. Denes, L. T. et al. Culturing C2C12 myotubes on micromolded gelatin hydrogels accelerates myotube maturation. *Skelet. Muscle* **9**, 17 (2019).
60. Ricotti, L. et al. Proliferation and skeletal myotube formation capability of C2C12 and H9c2 cells on isotropic and anisotropic electrospun nanofibrous PHB scaffolds. *Biomed. Mater.* **7**, 035010 (2012).

### Author contributions

H.B. and S.K. wrote the main manuscript text and prepared all figures. H.B., K.N. and S.K. reviewed the manuscript.

### Declarations

### Competing interests

The authors declare no competing interests.

### Additional information

**Supplementary Information** The online version contains supplementary material available at <https://doi.org/10.1038/s41598-025-01840-3>.

**Correspondence** and requests for materials should be addressed to S.K.

**Reprints and permissions information** is available at [www.nature.com/reprints](http://www.nature.com/reprints).

**Publisher's note** Springer Nature remains neutral with regard to jurisdictional claims in published maps and institutional affiliations.

**Open Access** This article is licensed under a Creative Commons Attribution-NonCommercial-NoDerivatives 4.0 International License, which permits any non-commercial use, sharing, distribution and reproduction in any medium or format, as long as you give appropriate credit to the original author(s) and the source, provide a link to the Creative Commons licence, and indicate if you modified the licensed material. You do not have permission under this licence to share adapted material derived from this article or parts of it. The images or other third party material in this article are included in the article's Creative Commons licence, unless indicated otherwise in a credit line to the material. If material is not included in the article's Creative Commons licence and your intended use is not permitted by statutory regulation or exceeds the permitted use, you will need to obtain permission directly from the copyright holder. To view a copy of this licence, visit <http://creativecommons.org/licenses/by-nc-nd/4.0/>.

© The Author(s) 2025